Research Article | Vol. 25, No. 15 | 24 Jul 2017 | OPTICS EXPRESS 17971
Optics EXPRESS

Active tracking system for visible light communication using a GaN-based micro-LED and NRZ-OOK

ZHIJIAN LU,[1,2,4] PENGFEI TIAN,[2,5] HONG CHEN,[1] IZAK BARANOWSKI,[1] HOUQIANG FU,[1] XUANQI HUANG,[1] JOSSUE MONTES,[1] YOUYOU FAN,[3] HONGYI WANG,[3] XIAOYAN LIU,[2] RAN LIU,[2] AND YUJI ZHAO[1,6]

[1]*School of Electrical, Computer and Energy Engineering, Arizona State University, Tempe, AZ 85287, USA*
[2]*Institute for Electric Light Sources, School of Information Science and Technology, Fudan University, Engineering Research Center of Advanced Lighting Technology, Ministry of Education, Shanghai, China*
[3]*Department of Microelectronics, Xi'an Jiaotong University, Xi'an 710049, China*
[4]*zhijianl@asu.edu*
[5]*pftian@fudan.edu.cn*
[6]*Yuji.Zhao@asu.edu*

Abstract: Visible light communication (VLC) holds the promise of a high-speed wireless network for indoor applications and competes with 5G radio frequency (RF) system. Although the breakthrough of gallium nitride (GaN) based micro-light-emitting-diodes (micro-LEDs) increases the -3dB modulation bandwidth exceptionally from tens of MHz to hundreds of MHz, the light collected onto a fast photo receiver drops dramatically, which determines the signal to noise ratio (SNR) of VLC. To fully implement the practical high data-rate VLC link enabled by a GaN-based micro-LED, it requires focusing optics and a tracking system. In this paper, we demonstrate an active on-chip tracking system for VLC using a GaN-based micro-LED and none-return-to-zero on-off keying (NRZ-OOK). Using this novel technique, the field of view (FOV) was enlarged to 120° and data rates up to 600 Mbps at a bit error rate (BER) of 2.1×10^{-4} were achieved without manual focusing. This paper demonstrates the establishment of a VLC physical link that shows enhanced communication quality by orders of magnitude, making it optimized for practical communication applications.

OCIS codes: (230.3670) Light-emitting diodes; (060.2605) Free-space optical communication; (060.4510) Optical communications.

References and links

1. H. Burchardt, N. Serafimovski, D. Tsonev, S. Videv, and H. Haas, "VLC: Beyond point-to-point communication," IEEE Commun. Mag. **52**(7), 98–105 (2014).
2. N. Zhao, X. Li, G. Li, and J. M. Kahn, "Capacity limits of spatially multiplexed free-space communication," Nat. Photon. **9**(12), 822–826 (2015).
3. P. Tian, J. J. McKendry, Z. Gong, S. Zhang, S. Watson, D. Zhu, I. M. Watson, E. Gu, A. E. Kelly, C. J. Humphreys, and M. D. Dawson, "Characteristics and applications of micro-pixelated GaN-based light emitting diodes on Si substrates," J. Appl. Phys. **115**(3), 1–6 (2014).
4. H. Chen, H. Fu, Z. Lu, X. Huang, and Y. Zhao, "Optical properties of highly polarized InGaN light-emitting diodes modified by plasmonic metallic grating," Opt. Express **24**(10), 856–867 (2016).
5. H. Chen, H. Fu, X. Huang, Z. Lu, X. Zhang, J. Montes, and Y. Zhao, "Optical Cavity Effects in InGaN Micro-Light-Emitting Diodes With Metallic Coating," IEEE Photon. J. **9**(3), 1–8 (2017).
6. M. S. Islim, R. X. Ferreira, X. He, E. Xie, S. Videv, S. Viola, S. Watson, N. Bamiedakis, R. V. Penty, I. H. White, and A. E. Kelly, "Towards 10 Gb/s orthogonal frequency division multiplexing-based visible light communication using a GaN violet micro-LED," Photon. Res. **5**(2), 35–43 (2017).
7. T. Peyronel, K. J. Quirk, S. C. Wang, and T. G. Tiecke, "Luminescent detector for free-space optical communication," Optica **3**(7), 787–792 (2016).
8. R. C. Peach, G. L. Burdge, T. Tidwell, and J. G. Vickers, "System and method for free space optical communication beam acquisition," U.S. Patent App. 13/780, 489 (2013).

#295943 https://doi.org/10.1364/OE.25.017971
Journal © 2017 Received 15 May 2017; revised 3 Jul 2017; accepted 4 Jul 2017; published 18 Jul 2017

Optics EXPRESS

9. M. Jeganathan, and K. Kiasaleh, "Transceiver, system, and method for free-space optical communication and tracking," U.S. Patent App. 09/808, 496 (2001).
10. H. Wang, T. Luo, Z. Lu, H. Song, and J. B. Christen, "CMOS self-powered monolithic light-direction sensor with digitalized output," Opt. Lett. **39**(9), 2618–2621 (2014).
11. H. Song, Z. Lu, T. Luo, J. B. Christen, and H. Wang, "A CMOS self-powered monolithic light direction sensor with SAR ADC," in *IEEE International System-on-Chip Conference* (IEEE, 2014), pp. 58–62.
12. H. Wang, T. Luo, Y. Fan, Z. Lu, H. Song, and J. B. Christen, "A self-powered single-axis maximum power direction tracking system with an on-chip sensor," Sol. Energ. **112**, 100–107 (2015).
13. W. Yang, S. Zhang, J. J. D. McKendry, J. Herrnsdorf, P. Tian, Z. Gong, Q. Ji, I. M. Watson, E. Gu, M. D. Dawson, L. Feng, C. Wang, and X. Hu, "Size-dependent capacitance study on InGaN-based micro-light-emitting diodes," J. Appl. Phys. **116**(4), 044512 (2014).
14. P. Tian, X. Liu, S. Yi, Y. Huang, S. Zhang, X. Zhou, L. Hu, L. Zheng, and R. Liu, "High-speed underwater optical wireless communication using a blue GaN-based micro-LED," Opt. Express **25**(2), 1193-1201 (2017).
15. V. Zabelin, D. A. Zakheim, and S. A. Gurevich, "Efficiency improvement of AlGaInN LEDs advanced by ray-tracing analysis," IEEE J. Quantum Electron. **40**(12), 1675–1686 (2004).
16. P. Tian, A. Althumali, E. Gu, I. M. Watson, M. D. Dawson, and R. Liu, "Aging characteristics of blue InGaN micro-light emitting diodes at an extremely high current density of 3.5 kA cm^{-2}," Semicond. Sci. Technol. **31**(4), 045005 (2016).
17. H. Fu, Z. Lu, and Y. Zhao, "Analysis of low efficiency droop of semipolar InGaN quantum well light-emitting diodes by modified rate equation with weak phase-space filling effect," AIP Adv. **6**(6), 065013 (2016).
18. H. Fu, Z. Lu, X. H. Zhao, Y. H. Zhang, S. P. DenBaars, S. Nakamura, and Y. Zhao, "Study of Low-Efficiency Droop in Semipolar (2021) InGaN Light-Emitting Diodes by Time-Resolved Photoluminescence," J. Display Technol. **12**(7), 736–741 (2016).
19. C. C. Pan, Q. Yan, H. Fu, Y. Zhao, Y. R. Wu, C. Van de Walle, S. Nakamura, and S. P. DenBaars, "High optical power and low-efficiency droop blue light-emitting diodes using compositionally step-graded InGaN barrier," Electron. Lett. **51**(15), 1187–1189 (2015).
20. C. A. Balanis, *Advanced Engineering Electromagnetics* (John Wiley & Sons, 2012).
21. J. R. Barry, J. M. Kahn, W. J. Krause, E. A. Lee, and D. G. Messerschmitt, "Simulation of multipath impulse response for indoor wireless optical channels," IEEE J. Sel. Areas Commun. **11**(3), 367–379 (1993).
22. J. M. Kahn, and J. R. Barry, "Wireless infrared communications," in *Proceedings of the IEEE* (IEEE, 1997), pp. 265–298.
23. J. B. Carruthers, and P. Kannan, "Iterative site-based modeling for wireless infrared channels," IEEE Trans. Antennas Propag. **50**(5), 759–765 (2002).
24. J. B. Carruthers, S. M. Carroll, and P. Kannan, "Propagation modelling for indoor optical wireless communications using fast multi-receiver channel estimation," in *IEEE Proceedings-Optoelectronics* (IEEE, 2003), pp. 473–481.

1. Introduction

The demand for high-throughput wireless communication has rocketed up over the past decade for the applications such as Internet of things (IoT), big data, augmented reality (AR), virtual reality (VR), and vehicle-to-vehicle communication. Although the fifth generation (5G) radio frequency (RF) communication network makes use of millimeter wave carrier frequencies up to 60 GHz, the limited frequency spectrum crisis restricts the development of wireless communication. To meet this challenge, free-space visible light communication (VLC) has emerged as a promising method for wireless communication [1]. The use of optical carrier frequencies allows for a dramatically wider available spectrum by many orders of magnitude, a high degree of spatial multiplexing, and the possibility to communicate at a higher data rate [2].

Light emitting diodes (LEDs) are commonly utilized as the optical source in VLC. Because the system bandwidth is primarily limited by the electrical to optical bandwidth of an LED, Gallium Nitride (GaN) based micro-LEDs become the popular choice for the VLC source. GaN based micro-LEDs' smaller carrier lifetime and lower junction capacitance scaled with their size lead to a bandwidth on the order of 100 MHz [3–5]. On-off keying (OOK), pulse-amplitude modulation (PAM) and orthogonal frequency division multiplexing (OFDM) have been used to achieve high-throughput communication up to 11.95 Gbps for one micro-LED [6], demonstrating the significant advantages of micro-LEDs in the application of VLC.

Due to the smaller size of a GaN-based micro-LED, the order of optical power decreases from 100 mW to 1 mW. Although this can be compensated for with focusing optics, the trade-off is a

Optics EXPRESS

reduced field of view (FOV) because of the conservation of etendue in geometrical optics. The loss of FOV associated with the constant increased active aperture is usually compensated for by active tracking systems in free-space optical communications [7–9]. Here, we present a method to increase the active area and FOV, which is widely used to concentrate light in solar energy harvesting. A new light tracking sensor and the needed circuit were integrated in a single chip which is fabricated by a standard 0.18 μm CMOS process. The results showed that the system has good sensitivity to the incident angle and achieve the tracking accuracy of 1.9° over a range of 120° [10, 11].

In this paper, we demonstrate an active tracking system, which consists of a motor and a CMOS chip with a light tracking sensor and the signal processing circuits [12]. Most of the circuits were integrated on the same chip to process the sensing signal and control the motor. This allows for high data rate visible light communication using a GaN-based LED and NRZ-OOK, insensitive to the spatial mode of the incident light achieving 600 Mbps at a bit error rate (BER) of 2.1×10^{-4} below the limit of forward error correction (FEC). For the indoor application, 3D high-definition (HD) video streaming to VR helmet requires high-speed wireless channels with radiation levels that would not pose a health threat. As a green communication link, the VLC system is employed to track the VR helmet movement and supply large volume HD video data. For the outdoor use, Facebook, Inc. conducts an innovate project named 'Connecting the World' [7]. As shown in Fig. 1, two unmanned flights are soaring in the sky within a 20 Km long range and connected by point-to-point VLC link using a laser diode (LD). This introduces a new set of challenges; the tracking system must be accurate enough to hit a dime-sized object from a distance of 20 Km. Air flow between the flights interferes with the point-to-point VLC link and necessitates the use of simultaneous active tracking.

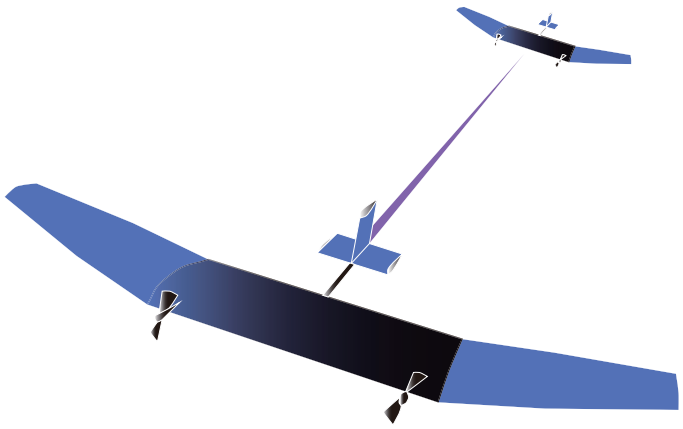

Fig. 1. For outdoor use, 20 Km long range point-to-point VLC link using an LD is needed in the latest project named 'Connecting the World' conducted by Facebook, Inc.

2. Experimental details

2.1. GaN-based micro-LED design and fabrication

We used a single GaN-based micro-LED with a pixel size of 80μm × 80μm. It was fabricated from a commercial LED wafer grown on a c-plane sapphire substrate. The LED had a typical p-i-n structure with an n-GaN layer, InGaN/GaN multiple quantum wells (MQWs), an AlGaN electron blocking layer, and a p-GaN layer. After Ni/Au (10nm/25nm) layers were deposited on top of the p-GaN, dry etching was employed to etch the Ni/Au layer and the GaN layers to form the mesas. P-contacts were generated by thermal annealing in purified air at 500 °C.

Optics EXPRESS

Then, SiO_2 was deposited by plasma-enhanced chemical vapor deposition as the passivation layer. Apertures on the mesas were further defined by HF-based wet etching. Finally, Ti/Au (50nm/200nm) deposited as the p-pad and n-pad to address each pixel separately. The micro-LEDs were packaged on a self-designed PCB and only the light emission from the sapphire side was used for VLC. The peak emission wavelength of the 80μm × 80μm micro-LED is approximately 440 nm at a driving current 40 mA [3]. To measure the -3dB modulation bandwidth of the packaged micro-LED, a small signal modulation from an Agilent N5225 network analyzer was combined with direct current from a Yokogawa GS610 source to drive the micro-LED. The emitted light was detected by a 1.4 GHz photodetector, after which the frequency response was read from the network analyzer.

2.2. The setup of VLC link

Figure 2 demonstrates the proposed VLC link using a single GaN micro-LED and NRZ-OOK, associated with an active pointing and tracking system. An Anritsu Signal Quality Analyzer MP1800A Pulse Pattern Generator generated high quality, low intrinsic jitter PN15 outputs up to 2.0 Vpp. A DC bias, GS610, was added to the AC input signal by a Bias-T, Mini-Circuits ZFBT-6GW, driving the blue GaN-based micro-LED. The light beam was focused by both transceiver and receiver lens in an 80 cm transmit distance and then captured by a 1.4 GHz bandwidth photodetector, HAS-X-S-1G4-SI-FS. The electrical output signal of the detector was tested by an Anritsu Signal Quality Analyzer MP1800A Error Detector and Wide-Bandwidth Oscilloscope 86100A to obtain BER and eye diagrams separately. In NRZ-OOK BER measurement, the delay model in MP18000A introduces a delay of N samples to the input signal, PN15 data pattern, to generate the reference. After the bit streams synchronization, the reference (REF) and test (TEST) inputs are compared for BER measurement.

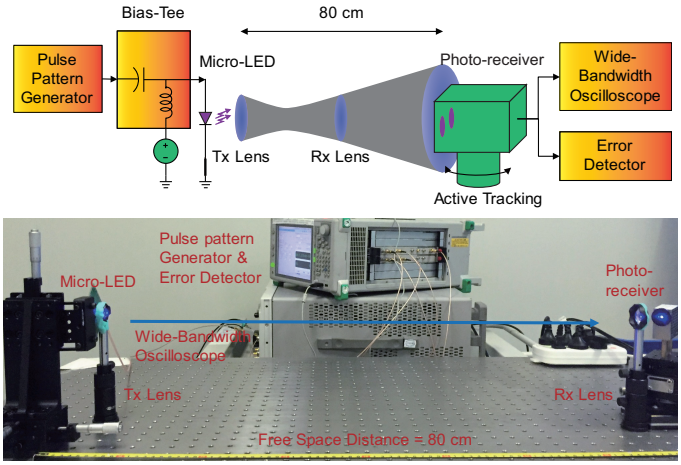

Fig. 2. Experimental setup including a VLC link using a GaN-based micro-LED and NRZ-OOK, an active tracking system using an on-chip photo sensor.

3. Results and discussion

3.1. Characteristics of GaN-based micro-LED

To evaluate the electrical and optical performance of the single 80 μm × 80 μm GaN-based micro-LED, we first packaged the die of micro-LED to high-speed printed circuit board (PCB) as shown in Fig. 3(a). It consists of a GaN-based micro-LED array, a high-speed PCB board,

Optics EXPRESS

and a soldered SMA connector. The modulation bandwidth saturates and is limited by the $R_{series}C_D$ time constant that is the product of LED's capacitance C_D and series resistance R_{series} under study [13]. The power-current (P-I) and voltage-current (V-I) response shown in Fig. 3(b) reveal that the sheet resistance $R_{series} = dV/dI$ at bias currents from 30 mA to 102.7 mA kept constant at approximately 19.1 Ω. When we exerted a small signal modulation to the current, it would induce the variation of the optical power. Because the P-I response is linear, the GaN-based micro-LED modulation performance is good for VLC. From the normalized electrical to optical frequency response of the GaN-based micro-LED as shown in Fig. 3(c), -3dB modulation bandwidth can be observed by increasing the bias current from 7.98 mA to 102.7 mA [14]. When bias current increases from 1 mA to 61 mA, the bandwidth shifts up rapidly. With the bias current higher than 61 mA, the bandwidth keeps constant around 160 MHz. Higher current causes more self-heating to the micro-LED, thus higher junction temperature degrades the micro-LED's lifetime and reliability dramatically [16–19]. Therefore, we chose 40.8 mA bias current and 4.6 V bias voltage for the operation point of VLC system, when the -3dB bandwidth of the micro-LED is 140 MHz. The electroluminescence spectrum test shows that the GaN-based micro-LED emits 440 nm wavelength blue light at the bias current of 40.8 mA.

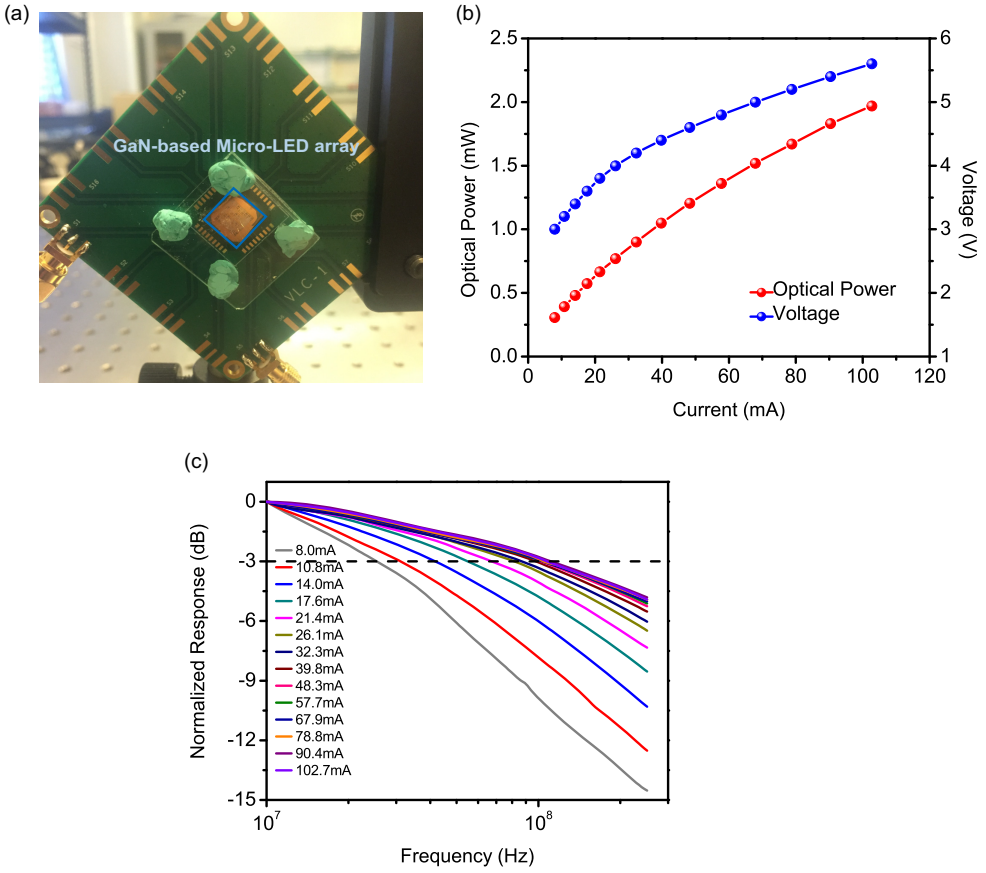

Fig. 3. Output characteristics of GaN-based micro-LED. (a) Image of the packaged 440-nm blue GaN-based micro-LED. (b) P-I curve and V-I curve of the GaN-based micro-LED. (c) Frequency responses of the GaN-based micro-LED at different bias currents from 7.98 mA to 102.7 mA.

Optics EXPRESS

3.2. 440-nm blue micro-LED based VLC system over an 80-cm free space distance

With an active tracking system using an on-chip photo sensor, a VLC link using a GaN-based micro-LED and none-return-to-zero on-off keying (NRZ-OOK) is experimentally set up as shown in Fig. 2. Since the blue GaN-based micro-LED is employed as both a lighting source and a data transmitter in the VLC system, most of the light emission is distributed within a large angle of approximately 120° [15]. Because of its smaller optical power compared to LEDs and Laser diodes, the light emission is collimated by the focusing lens to ensure that the most optical power can hit the PIN receiver. As a trade-off, its low divergence angle after collimation inevitably limits the allowable lighting range. Therefore, the focusing lens placed next to GaN-based micro-LED would correspond to the carried data quality, and it also affects its divergence angle. It means that the transmission performance of VLC link would depend on the direction of the measurement setup which was placed with respect to the GaN-based micro-LED. In this work, the active tracking system adhered to the photo receiver is placed in front of the blue micro-LED with a free-space distance of 80 cm to investigate its maximal allowable transmission capacity. 80 cm is a limiting distance because of collimation issue. We expect that a longer distance over 5 m can be feasible in our future work after optimizing the optical antennas. Optics techniques are employed to collimate the micro-LED light beam for the transmitter and focus the beam for the receiver.

For VLC link using GaN-based micro-LED and NRZ-OOK, manual focus offers the high-speed and high-quality wireless communication demonstration within 80-cm free-space transmit distance. NRZ-OOK is applied, and eye diagrams are as shown in Fig. 4. Error free eye diagrams at 200 Mbps, 300 Mbps, 400 Mbps, and 500 Mbps could be acquired at 40.8 mA DC bias. In Fig. 5(a), the BER at different driving currents was tested from 13.2 mA to 101.8 mA. A higher data communication speed can be achieved at a higher driving current, due to the increase of modulation bandwidth and light output power. From 70 mA to 101.8 mA, a slightly higher speed than 600 Mb/s was achieved, as the bandwidth already saturated at 70 mA. At 78 mA, a data rate of 600 Mb/s was obtained with a BER 3.4×10^{-7} (below FEC 3.8×10^{-3}). Although manual focus leads to good performance in VLC, at 40.8 mA within 80-cm free-space transmit distance, the received power is 1.15 mW. At data rates of 200 Mbps, 300 Mbps, and 400 Mbps, BERs are below than 1×10^{-13}. Therefore, the NRZ-OOK VLC link is error free. At data rates of 500 Mbps and 600 Mbps, BERs are 1×10^{-10} and 2.1×10^{-4}, separately as shown in Fig. 5(b). We employ neutral density filters to fade the received power to a fourth for VLC BER measurement. Figure 5(b) shows the trend that BER drops exponentially to 2.8×10^{-3} at 500 Mbps when the received power decreases to its one-fourth. Because the received power decreases, then the received effective signal intensity becomes less. So the signal to noise ratio (SNR) and BER become worse.

3.3. Active tracking system

An on-chip CMOS sensor aims to track the incident light and point in the direction of the light. Figure 6(a) shows an elementary cell of the sensor. The whole sensor is formed by a set of the basic cells. A metal wall created by stacking all metal layers, contacts, and vias available in the process is used to generate the on-chip micro-scale shadow. The height of the metal wall is H. The height is imposed by the metal stack. Because of the standard CMOS process, there are only a few choices of the photo sensor's dimensions. We optimize the dimensions of the metal wall for the sensor's performance considering a trade-off between field of view (FOV) and precision [10–12]. In this design, we choose 12 μm as the height of the metal wall. Diffraction has been considered. The bandgap voltage of silicon is about 1.12 V. Thus, the sensor can absorb the light wavelength up to 1.1 μm, which covers 440 nm blue light generated by GaN-based micro-LED. However, the distance between two adjacent metal walls is 30 μm, and the height of the metal wall is 12 μm. The physical dimensions are much larger than the wavelength

Optics EXPRESS

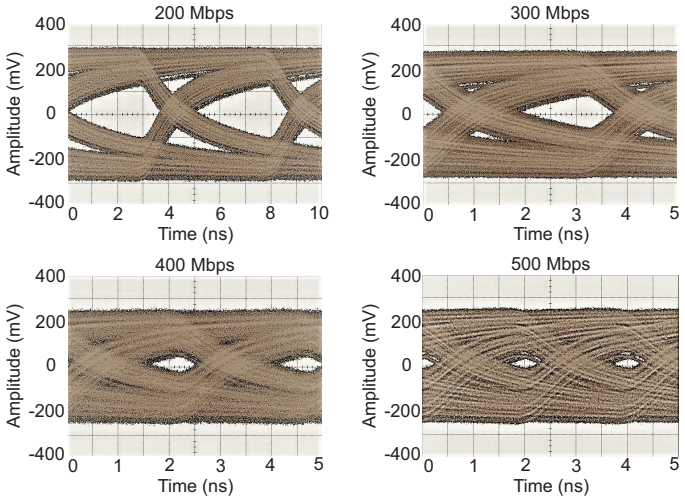

Fig. 4. Open eye diagrams with 200 Mbps, 300 Mbps, 400 Mbps, and 500 Mbps acquired at 40.8 mA DC bias.

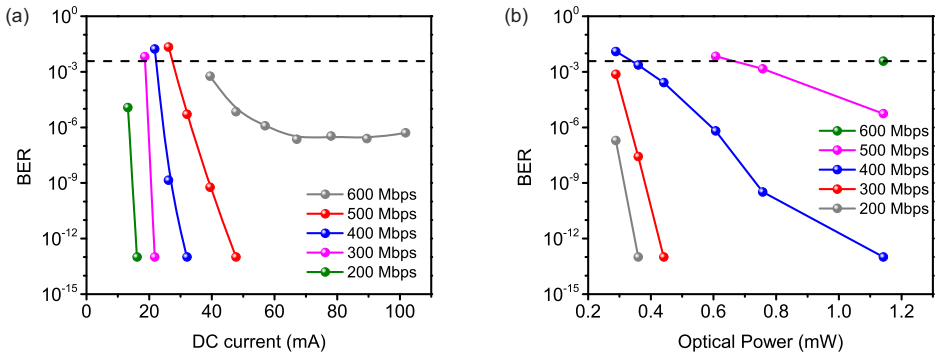

Fig. 5. (a) The BER at different bias current. (b) The BER at different received optical power.

of the absorbed light, so the diffraction has little impact on the sensor's performance.

Two identical photodiodes are located on opposite sides of the metal wall. D_L is the left side diode and D_R the right side diode. They have the same width W and the same length L. The schematic current sources shown beside each diode indicate the photocurrents generated by the corresponding photodiodes. The angle between the metal wall and the light direction is θ. When the light comes from directly above of the wall, namely $\theta = 0$, the two photodiodes are illuminated equally and produce the identical current values. When the light comes from one side above the wall, namely $\theta > 0$ or $\theta < 0$, the wall blocks part of the light to the opposite photodiode will produce less current than the other photodiode. So the relationship between of I_L and I_R is relative to the incident light angle θ given by [12]

$$\frac{I_L}{I_R} = \begin{cases} \dfrac{(1+\beta)L \cdot \cos\theta + \alpha H \cdot \sin\theta}{(1+\beta)L \cdot \cos\theta - H \cdot \sin\theta}, & \theta \geq 0 \\ \dfrac{(1+\beta)L \cdot \cos\theta + H \cdot \sin\theta}{(1+\beta)L \cdot \cos\theta - \alpha H \cdot \sin\theta}, & \theta < 0 \end{cases} \tag{1}$$

Optics EXPRESS

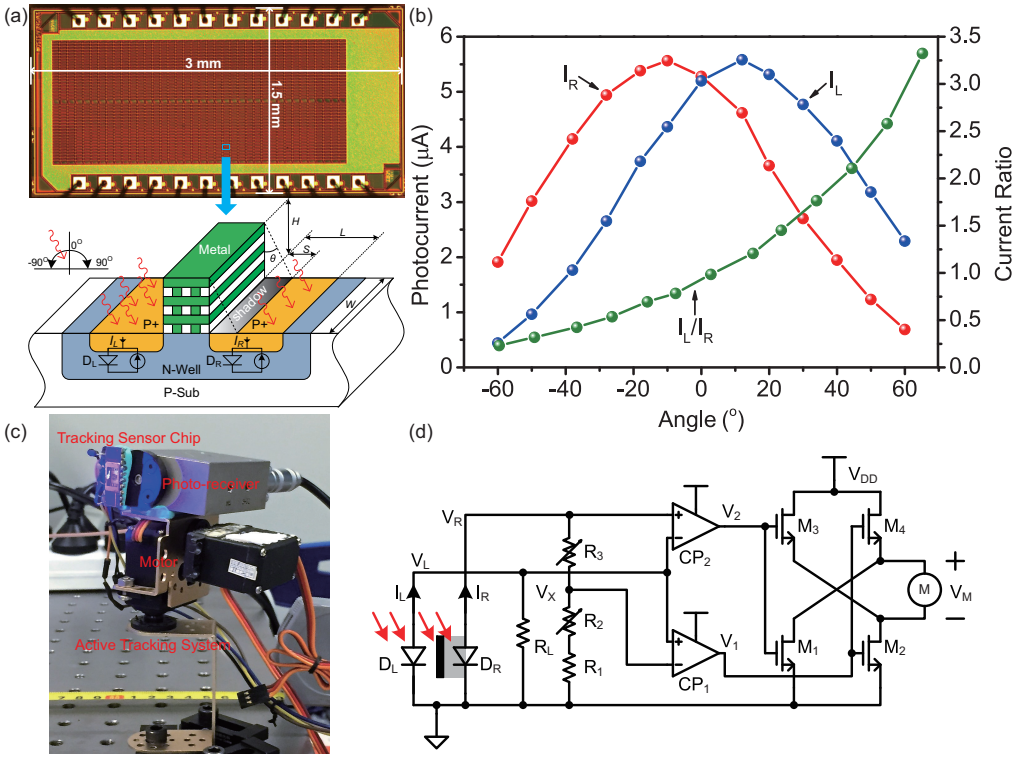

Fig. 6. (a) On-chip light tracking sensor structure and micrograph. (b) Photocurrents and Current ratio versus incident light angles under the power density of 80 mW/cm^2. (c) Photograph of the active tracking system. (d) Block diagram of the proposed tracking circuit.

where α corresponds to the ratio of the reflected light to the total light reaching the left side of the metal wall, β corresponds to the ratio of the reflected light to the total light reaching the right side of the metal wall. Since α and β depend on the process, layout, and package, their values are assumed to be constant in a given design. Therefore, from Eq. (1) we can see the current ratio of I_L/I_R is independent of the light intensity and only depends on the incident light angle θ. Figure 6(b) demonstrates the photocurrents I_L, I_R and its current ratio versus the angle of the incident light under the constant light intensity of 80 mW/cm^2. It was tested with KEITHLEY 2636A Source Meter. Both photocurrents change with the light angle. When the angle is zero, I_L and I_D are almost the same. When the light comes from left side $\theta < 0$, $I_L > I_R$ and when the light comes from right side $\theta > 0$, $I_L > I_R$.

The active tracking system for VLC contains an on-chip light tracking sensor, the integrated signal processing circuits, a motor, and the mechanical transmission as shown in Fig. 6(c). We utilized separate receivers for data and tracking, which are attached side by side as also shown in Fig. 6(c) to ensure that both of their maximum received optical power points are identical. Figure 6(d) shows the circuit of the tracking system. Although motors are servo motors controlled by PWM, we changed the servo motors into DC motors. Therefore, they respond to voltage differentials to make the feedback system simple and reliable. Photodiodes D_L and D_R and photocurrents I_L and I_R are the same as shown in Fig. 6 (b). It can be seen when $\theta < \theta_1$, the motor is driven by $V_M > 0$, the angle will increase. When $\theta > \theta_2$, the motor is driven by $V_M < 0$ and the angle will decrease. When $\theta_1 < \theta < \theta_2$ and $V_M = 0$, the motor will be stationary and there will be no power consumed by the motor driver. This is the stable region. In this design, the static consumed current is only 88 μA for the low power applications. The tracking module

Optics EXPRESS

consumes 334 mA during the operation. The results showed that the system has good sensitivity to the incident angle and achieve a tracking accuracy of 1.9° over a range of 120°.

3.4. *An active tracking system for 440-nm blue micro-LED based VLC system over an 80-cm free space distance*

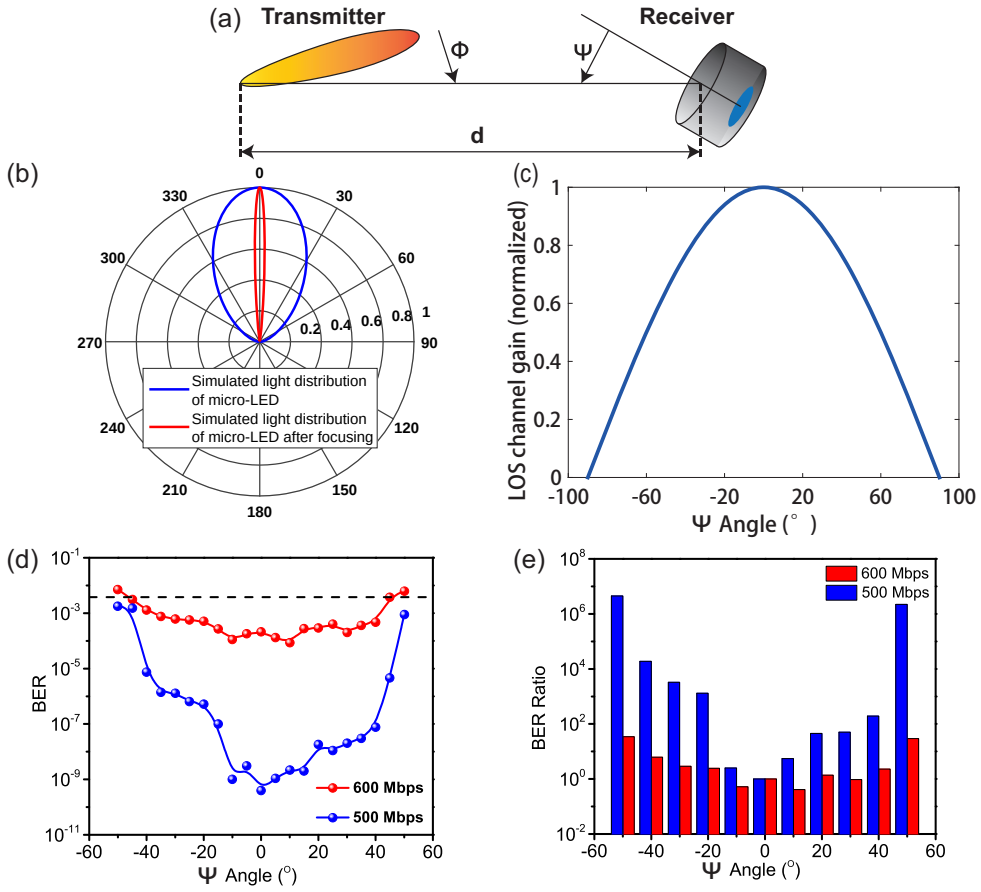

Fig. 7. (a) LOS geometry used in channel gain calculations. (b) Simulated light distribution of micro-LED and its distribution after focusing versus the angle of irradiance. (c) Simulated normalized LOS channel gain versus the angle of incidence when the angle of irradiance is fixed. (d) The BER for different angle of incidence at data rates of 500 Mbps and 600 Mbps. (e) Active tracking system improved VLC performance at data rates of 500 Mbps and 600 Mbps.

LOS geometry used in micro-LED light distribution simulation and LOS channel gain simulation is demonstrated in Fig. 7(a), where d is the free space distance between the GaN-based micro-LED and the PIN receiver; ϕ is the angle of irradiance; and ψ is the angle of incidence. In order to estimate the farfield of a micro-LED manipulated by the focal lens, a simple ray optics approximation is used [20]. It is noted that this approximation is only accurate when $tan\phi \approx \phi$, which is clearly not always the case in our experiment. However, since the most of power is concentrated at small ϕ region, this approximation still provides valuable information for this research. To approximate the farfield from a micro-LED, a Gaussian-type distribution is used in Eq. (2), where R is the radiance; ϕ is the angle of irradiance; and ϕ_0 is the fitting parameter

Optics EXPRESS

assumed as 30° in this work. The farfield pattern is shown in Fig. 7(b) (blue curve).

$$R(\phi) = exp(-\frac{\phi^2}{2\phi_0^2}) \tag{2}$$

By implementing a simple ABCD matrix method in ray optics shown in Eq. (3), the farfield and energy distribution can be solved, where y_0 and ϕ_0 indicate the initial position and the initial angle. In this calculation, y_0 is 0 and ϕ_0 is calculated by Eq. (2). The M matrix is determined by Eq. (4), whose value for each component can be found in Table 1. B_1 represents the distance between the micro-LED and the focus lens; C_2 represents the lens strength; and B_3 represents the distance between the micro-LED and the PIN receiver. The calculated farfield and power distribution is shown in Fig. 7(b) (red curve).

$$\begin{bmatrix} y_1 \\ \phi_1 \end{bmatrix} = M_1 M_2 M_3 \begin{bmatrix} y_0 \\ \phi_0 \end{bmatrix} \tag{3}$$

$$M_i = \begin{bmatrix} A_i & B_i \\ C_i & D_i \end{bmatrix} \tag{4}$$

Table 1. ABCD matrix value

i	A_i	B_i	C_i	D_i
1	1	0.55 cm	0	1
2	1	0	-2 cm^{-1}	1
3	1	80 cm	0	1

LOS channel gain is given by Eq. (5). [21–24]

$$H(0)_{LOS} = \begin{cases} \frac{(m+1)A}{2\pi d^2} cos^m(\phi) T_s(\psi) g(\psi) cos(\psi), & 0 \le \psi \le \Psi_c \\ 0, & \theta > \Psi_c \end{cases} \tag{5}$$

where $m = -\frac{ln2}{ln(cos(\Phi_{1/2}))}$ is the Lambertian order of the optical source related to $\Phi_{1/2}$, the transmitter semi-angle (at half power). Typical directed transmitter $\Phi_{1/2} = 15°$ corresponds to $m = 20$. A denotes the detection area of the PIN receiver. We also assume that the receiver is pointed straight upward, and employs a concentrator of half-angle FOV $\Psi_c \approx 50°$ that achieves omnidirectional gain $g(\psi) \approx g \approx n^2$ and an omnidirectional filter having $T_s(\psi) \approx T_s$. We did simulation based on those equations and got results of normalized LOS channel gain versus the angle of incidence ψ when the angle of irradiance ϕ is small as shown in Fig. 7(c). The LOS channel gain is proportional to the received optical power. If ϕ is kept very small, we can increase $H(0)$ by narrowing the angle ψ, which enhances the SNR or BER of this VLC system. In addition, the active tracking system aims to track the maximum power point. The simulation results show that the tracking system will enhance the received optical power, the SNR or BER of this VLC system when the communication system is aligned.

Figure 7(d) shows that the BER becomes worse exponentially when the incident light comes away from the point-to-point link. It proves that the angle of incidence changes the concentration of the received power, similar to the mechanism using neutral density filter as shown in Fig. 5(b). So, the active tracking system is essential in VLC, especially for practical indoor or outdoor applications. The histogram as shown in Fig. 7(e) illustrates that the active tracking system enhances VLC performance if it is out of focus or away from the point-to-point transmission. BER ratio denotes the ratio of the BER with active tracking to the BER without active tracking. When the angle is 0°, BER ratio is 1 because active tracking system does not work to change the

Optics EXPRESS

direction of the PIN receiver. Within a 10° range, BER does not improve dramatically even if the active tracking system works because the ball lens of the PIN receiver already concentrates the received optical power. In the range from 10° to 50°, BER improves exponentially by automatically narrowing the angle of incidence. When the angle of incidence is between 50° and 60° out of half-angle FOV, active tracking system can still sense the incident light and narrow the angle of incidence to provide a valid VLC link.

For the future research, we aim to achieve a two-axis active tracking system for VLC link, which provides a more realistic scenario to LOS VLC link in the free space. It seems impossible to do manual alignment in that scenario.

4. Conclusion

VLC can be used to realize a high-speed wireless network capable of competing with 5G RF systems. Additionally, GaN-based micro-LEDs offer key qualities ideal for the implementation of VLC applications. The VLC using GaN-based micro-LED shows the communication link at a data rate of 600 Mbps and a BER of 2.1×10^{-4} within a distance of 80 cm in our work. However, this VLC system is so sensitive that manual focus is necessary. We demonstrated an active tracking method to increase BER by orders and enlarge the FOV of the PIN receiver to 120° when it is out of focus. Therefore, the micro-LED based VLC becomes both mechanically and optically robust. Future research will be focused on developing integrated optics on the PIN receiver in cooperation with active tracking.

Funding

Bisgrove Scholar Program from Science Foundation Arizona; National Natural Science Foundation of China (61571135); Fudan University Start-up Research Funding.